PCCP

Accepted Manuscript

Journal Name

Dynamic Article Links ▶

ARTICLE TYPE

Physical Chemistry Chemical Physics Accepted Manuscript

DFT/TDDFT investigation on the UV-vis absorption and fluorescence properties of alizarin dye

Anna Amat,*[a] Costanza Miliani[b,c] Aldo Romani[c,b] and Simona Fantacci*[a]

The photophysical and photochemical properties of alizarin, a fluorescent organic red dye of the family of the anthraquinones, have been theoretically investigated, focusing our attention on the emission properties in relation to an excited state internal proton transfer from the phenolic hydroxyl group to the carbonylic oxygen. The potential energy curve of the proton transfer in the first excited state has been
10 computed in solvents of different polarity and the emission spectra of both tautomers simulated including the vibronic effects by means of the FC approximation. Calculations performed equilibrating the solvent with the excited state geometry and electron density by means of a self-consistent procedure have lead to interesting differences with respect to their linear response counterpart. The results obtained point out that, while the emission energy of alizarin is sensitive to the solvent polarity, that of the proton-transfer
15 tautomer is computed at similar wavelengths independently of the medium. The comparison between the computed and the experimental data has allowed us to rationalize the alizarin double emission measured in non-polar solvents.

Introduction

Anthraquinones are a family of organic compounds widely used
20 for their pharmaceutical properties.[1-4] Among them, the hydroxyanthraquinones (HAQ), extracted from the roots of plants belonging to the Rubiaceae family, are brightly coloured derivatives that have been used as dyes since antiquity due to their strong absorption in the visible and their availability.[5-10]
25 Alizarin (1,2-HAQ), see Scheme 1, is a natural occurring hydroxyanthraquinone that, together with purpurin (1,2,4-HAQ), constitutes the main colouring matters of madder. Extracted from Rubia tinctoria L., madder was one of the most popular dyestuffs and was used to dye textiles and as a red lake in paintings by
30 precipitation of the water extract with metal salts. Nowadays, alizarin is currently prepared synthetically, and in the last years it has also been used as a sensitizer for dye-sensitized solar cells (DSC).[11-20] Due to the great interest in the chromatic properties of alizarin, for different application fields, its photophysics and
35 photochemistry have been widely investigated.

It is well-known that computational simulations can play an important role in describing the relationships between structural and optical properties at the ground and excited states.[21-25] Advances in this field, as the possibility to compute TDDFT
40 analytical gradients in solvent[26,27] and the inclusion of vibronic contributions to the computed spectra,[28-32] according to the Frank-Condon theory, had recently lead the excited state calculations to accuracies similar to those of the ground state. Several computational studies exploiting DFT and TDDFT
45 methodologies to investigate alizarin compounds have been reported previously. In particular, the structural and electronic
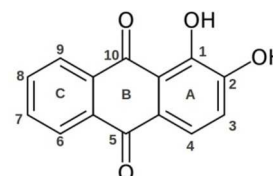
Scheme 1 Alizarin structure and numbering scheme

properties of the ground state and the electronic absorption
50 spectra of alizarin[33-36] and alizarin metal complexes have been investigated[36-39] and the interaction of alizarin with TiO$_2$ surfaces studied in the framework of DSC.[11-20] Recently, the Frank-Condon theory has been used to compute vibrationally-resolved spectra to study the absorption spectra of alizarin[36] and
55 the absorption and emission spectra of the umbelliferone–alizarin bichromophore,[40] allowing for a more meaningful comparison between the simulated and the experimental data.

Many natural organic dyes show peculiar fluorescence properties, i.e. excited state internal proton transfer (ESIPT), wavelengths
60 dependent emissions, and/or important solvatochromic effects that makes them suitable for a large number of applications. In particular, alizarin presents a broad absorption band at ca. 430 nm[41-44] and a weak emission at ca. 640 nm[44,45] that gives rise to a large Stokes shift suggesting a marked change in the molecular
65 geometry of the excited state that was ascribed to an excited state internal proton transfer.[44] A slightly different emission behaviour in different solvents was also reported in Ref. [44] with a wavelength dependent double emission measured in benzene and a single broad band in polar solvents. In particular, in
70 benzene, exciting at 465 nm a double emission with peaks at 565

and 610 nm and a low intensity shoulder at ca. 660 nm were measured. Exciting at higher energies the high energy band lowered in intensity while the low energy band became less sharp and was red-shifted. On the other hand, in acetonitrile and ethanol

5 solvents a broad band with a plateau-like maximum between 610 and 660 nm was measured thus hypothesizing the emission originating only from the proton transfer tautomer.[44] Alizarin has been used in this investigation to setup a methodology for the calculation of the emission properties that can be then generally

10 extended to the study of different organic dyes presenting a similar behaviour. Moreover, the comprehension of alizarin double emission can be relevant both in the cultural heritage field, for identification purposes, and in the DSC field to design new dyes with optimized target functionalities.

15 In the present paper, we will briefly discuss the alizarin absorption spectra, while we mainly focus on the emission of alizarin, the occurrence of an internal excited state proton transfer and the dependence of these phenomena on the solvent. As a first step, the structural and electronic properties of alizarin in the

20 ground (S_0) and first excited (S_1) state have been studied in different media. Either alizarin (ALZ), see Scheme 1, and its proton transfer tautomer (ALZ_PT) have been found stable both on the ground and first excited state. To get insight into the proton transfer process, the potential energy curve as a function

25 of the proton-transfer $O_{10}H$ coordinate has been computed and the excited-state barrier energy of the tautomerization analysed. The optical properties of both tautomers have been also investigated, focusing our attention on the photophysics of the excited state. The emission spectra including the vibronic effects

30 have been computed and compared to the available experimental data to rationalize the double emission measured in benzene and the changes observed with the increase of the solvent polarity. Two different procedures for the inclusion of solvation effects with a polarizable continuum model (PCM) in the excited states

35 have been evaluated: the linear response (LR-PCM) and the state specific[46-48] one (SS-PCM) where the solvent is equilibrated with the excited state electron density by means of a self-consistent procedure. The obtained results point out that both procedures lead to significantly different results, and that they

40 have a noticeable impact not only on the computed stabilities, but also on the structural properties of the excited states.

Computational Details

All the calculations have been performed with DFT[49] and its Time-Dependent extension TDDFT[50-52] as implemented in

45 Gaussian09 (G09) program package,[53] using B3LYP[54-56] as exchange-correlation functional and 6–31g** basis set.[57,58] Solvation effects have been included by means of PCM,[46] as implemented in G09. Optimizations of the excited states have been performed using a linear response (LR-PCM) approach. To

50 get a more accurate description of the solvent effects in the excited state, the solvent reaction field has been equilibrated to the excited state electron density using a state specific self-consistent procedure (SS-PCM)[47,48] on the optimized LR-PCM structures. This procedure should provide in principle to a better

55 description of the solute-solvent interactions in the excited state.[21,47,48]

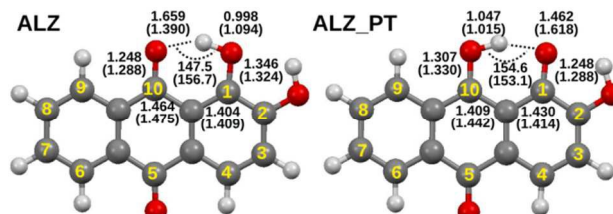The potential energy curves related to the proton transfer in the

Figure 1 Optimized molecular structures of ALZ (left) and ALZ_PT
60 (right). The main geometrical parameters (bond length in Å and angles in degrees) computed in benzene in the ground (first excited state).

excited state have been computed by freezing the distance between the proton and the carbonylic oxygen in position 10 (O_{10}) of the B-ring, see Figure 1. $O_{10}H$ distances have been fixed

65 in steps of 0.050 Å ranging from 0.850 Å to 1.850 Å while the rest of the coordinates have been freely optimized. SS-PCM calculations have been performed on the obtained optimized structures to equilibrate the solvent with the solute geometry, thus computing different potential energy curves.

70 The vibrationally resolved emission spectra have been computed using the Franck-Condon approximation within the adiabatic Hessian approach by means of the FC Classes code as implemented in G09.[29-32] This approach is quite time-demanding as both states are treated at the same level of calculation and

75 optimization and frequency calculations have to be performed for both the ground- and excited-state. Analytical frequency calculations are used in the ground state while for the excited state first and second derivatives are computed analytically and numerically, respectively. The numerical second derivatives are

80 performed by applying finite differences to the three cartesian coordinates of each atom on the excited state geometry thus resulting in a total number of 6N+1 analytical first derivative calculations, being N the number of atoms in the molecule. Since temperature dependant calculations have not yet been included in

85 the implementation of G09 used in this work, the progression of the spectrum coming from different populated states is simplified to a series of transitions coming from the ground state of the electronic state of interest (<0|vi'>).

All the computed emission spectra have been convoluted with a
90 Lorentzian function using a full width at half maximum (FWHM) of 600 cm^{-1} to fit the experimental shape.

Molecular structure

The molecular structure of alizarin and its possible photo-tautomer have been optimized at ground (S_0) and first excited

95 states (S_1), see Figure 1. Geometry optimizations performed in vacuo, ethanol and benzene provide stable tautomers in both states. The presence of a stable proton transfer tautomer in S_0 is in contradiction with previous calculations by Preat et al.,[33] that reported no stable proton transfer tautomer in water while it was

100 found stable by Carta et al.[36] We performed frequency calculations on the optimized structures, finding all positive frequencies in all the different media, confirming therefore that the structures for both tautomers are real minima, consistently with experimental stability data.[59]

105 Calculations performed in the different media do not show relevant differences in the optimized structural parameters. Figure 1 reports the main distances and angles optimized in benzene,
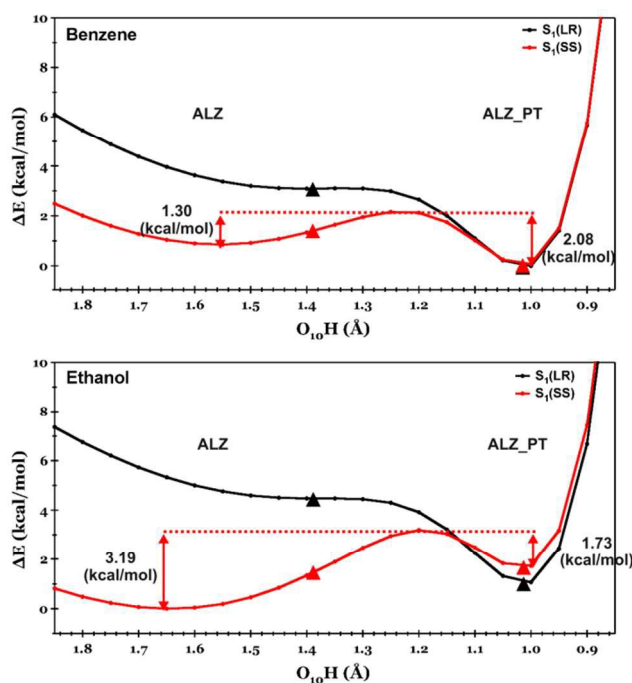
Figure 2. . Potential S_1 energy curves as a function of the $O_{10}H$ distance computed in benzene (top) and ethanol (bottom). The red and black lines are obtained using the LR and SS approaches, respectively. ▲ and ▲ markers indicate the LR and the SS stabilities computed on the freely optimized LR geometries, respectively

while the results in vacuo and in ethanol are collected in the Electronic Supplementary Information (ESI).

In the ground state the only noticeable differences between ALZ and ALZ_PT optimized geometrical parameters are retrieved in the distances and angles between the atoms involved in the proton transfer. CO_{10} distance increases as expected when passing from the carbonyl (ALZ) to the alcoholic configuration (ALZ_PT) while the contrary is true for the $C-O_1$ distance. When the proton is bound to O_1 (ALZ) the OH bond length is shorter than when bound to O_{10} (ALZ_PT) reflecting the major acidity of O_{10} with respect to O_1. On the other hand, the O_1HO_{10} angle increases of ca. 10° in the proton transfer tautomer.

For ALZ the main differences going from the ground to the S_1 excited state are retrieved on the distance $O_1(O_{10})H$ that decreases(increases) of ca. 0.1(0.3) Å while the O_1HO_{10} angle opens by ca. 10°. For ALZ_PT we observe an opposite trend, a lengthening of the O_1H bond by ca. 0.2 Å and the shortening of the distance between the proton and the carbonyl oxygen $O_{10}H$, while the O_1HO_{10} angle is almost unchanged with respect to the ground state geometry.

The relative stabilities of both tautomers computed in the ground state show that the ALZ tautomer is 4.83/4.81/4.78 kcal/mol more stable than ALZ_PT in vacuo/benzene/ethanol. To compute the S_1 relative stabilities in solution, the solvent has been equilibrated to the excited state electronic distribution on the LR-PCM optimized S_1 geometries. ALZ_PT is computed 2.89/1.40 kcal/mol more stable than ALZ in vacuo/benzene while in ethanol the two tautomers are almost isonergetic, with ALZ found more stable by only 0.20 kcal/mol. Attempts to locate the transition states structures between the two tautomers using the LR-PCM optimization failed. Therefore, the potential energy

curves in the excited state along the proton transfer coordinate have been computed for both tautomers.

The molecular structures were optimized in the first excited state at different fixed $O_{10}H$ distances. On each constrained optimized molecular structure a SS-PCM calculation was performed to equilibrate the solvent with the excited state electronic density, the obtained results are reported in Figure 2. By using the SS-PCM approach, the apparent charges that characterize the solvent are equilibrated with the computed charge distribution of the state of interest and not with the transition charge density as in the LR-PCM case. Therefore, this procedure is more appropriate to investigate geometrical relaxation of the exited states as shown for the 1-hydroxy-2-methoxy-anthraquinone.[40]

Interestingly, we notice that the LR-PCM calculations do not report any consistent barrier in the proton transfer pathway which explains the failure to locate the transition state. Only the ALZ_PT are real minima in the S_1 respectively. Surprisingly, in ethanol the ALZ is computed 1.46 kcal/mol more stable than ALZ_PT and the barrier height is computed 3.19 kcal/mol and 1.73 kcal/mol with respect to the ALZ and the ALZ_PT tautomers. It has to be pointed out, considering the protic nature of the solvent, that specific solute-solvent interactions might be present and influence the ESIPT process. These interactions are neglected in our approach even though they might similarly count for both tautomers. To check this effect and to disentangle the H-bondig effects from the polarity of the solvent, we repeated the same calculations on ALZ and ALZ_PT using acetonitrile as solvent. Moreover, the choice to perform calculations in acetonitrile is justified by the fact that and the optimized ALZ structures correspond to a flat region of the energy curve around between $O_{10}H$ = 1.5 and 1.3 Å. The optimized LR-PCM ALZ structures have been reported with triangle markers on Figure 2. On the contrary, the energy curves computed using the SS-PCM method show two clear minima corresponding to the ALZ and the ALZ_PT tautomers and a non-negligible barrier height. The ALZ minima are found at $O_{10}H$ = 1.550 and 1.650 Å in benzene and ethanol, respectively, different from the 1.390 Å value computed with the LR-PCM optimization in both solvents.

In benzene the ALZ_PT minimum is located 0.80 kcal/mol below that of ALZ and barrier heights of 1.30 and 2.08 kcal/mol are computed for the proton and the back-proton transfer, experimentally the emission spectra of alizarin measured in ethanol and acetonitrile show the same main features. It is worth noting that both the LR-PCM and SS-PCM energy potential curves of the ESIPT process in acetonitrile are very similar to those computed in ethanol (see ESI for further details). In acetonitrile, the ALZ is computed 1.83 kcal/mol more stable than ALZ_PT and the barrier height is computed 3.24 kcal/mol and 1.41 kcal/mol with respect to the ALZ and the ALZ_PT tautomers. We therefore find that the most stable species in the lowest excited state in polar solvent is the ALZ and that its relative stability increases by increasing the polarity of the solvent. To check the reliability of the functional and basis set used in our calculations, the relative stabilities of the SS curve minima structures have been also computed using PBE0[61] and M06[62,63] and an extended basis set (6-311++G**). The results obtained (see ESI) confirm the relative stabilities computed using B3LYP/6-31G**, i.e. the major stability of ALZ and ALZ_PT in

Table 1 ALZ and ALZ_PT main computed transitions, oscillator strength (f) and composition in terms of molecular orbitals in vacuo and in different solvents.

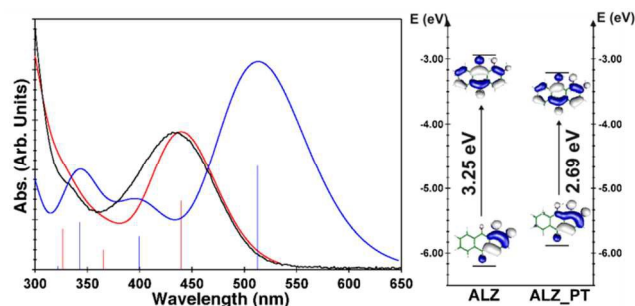|	ALZ			ALZ_PT		
	Trans. nm (eV)	f	MO	Trans. nm (eV)	f	MO
Benz.	440 (2.81)	0.136	98% H→L	520 (2.38)	0.206	98% H→L
DMSO	440 (2.82)	0.138	97% H→L	513 (2.42)	0.208	98% H→L
Eth.	439 (2.83)	0.134	97% H→L	512 (2.42)	0.202	98% H→L
Vac.	435 (2.85)	0.092	97% H→L	511 (2.45)	0.140	97% H→L

Figure 3 Computed absorption spectra in DMSO for ALZ (red) and ALZ_PT (blue) compared to the experimental absorption spectrum of alizarin in a mixture of DMSO:water (50:50).[42] Right: ALZ and ALZ_PT frontier molecular orbitals energies and isodensiy plots computed in DMSO

ethanol and in benzene, respectively.

As a general conclusion, the comparison between the LR-PCM and the SS-PCM results points out the importance of the solvent equilibration in the excited state. Not only different potential energy curves are computed but also the geometrical structures of the minima are different, with the $O_{10}H$ distance in the ALZ minima of the SS-PCM and LR-PCM potential energy curves varying by as much as 0.2 Å.

Absorption spectra

The absorption spectra of both tautomers in different media have been computed. Results are reported in Table 1 and comparison with the experimental data in DMSO is reported in Figure 3. In all the calculations, the main absorption band of ALZ is originated by a single HOMO→LUMO transition computed in between 440 and 435 nm depending on the media. The obtained results are in good agreement with the experimental data[43,60] and with previous theoretical calculations.[33,59] The ALZ_PT absorption spectra, originated by an intense HOMO→LUMO transition computed between 520-511 nm, also shows a very small response to the media with small blue-shifts with the increase of the solvent polarity. As can be noticed from Figure 3, the computed spectra of ALZ in DMSO is in good agreement with the experiment. On the contrary, the computed spectra of ALZ_PT is rigidly red-shifted with respect to the experiment. The absence in the experimental spectrum of absorption features above 500 nm completely rules out the involvement of ALZ_PT in the measured electronic absorption spectrum, consistently with the computed relative stability for the two tautomers at the ground state. Other experimental investigations report the presence of a low intensity shoulder in the absorption spectrum that has been assigned to the ALZ_PT tautomer.[59]
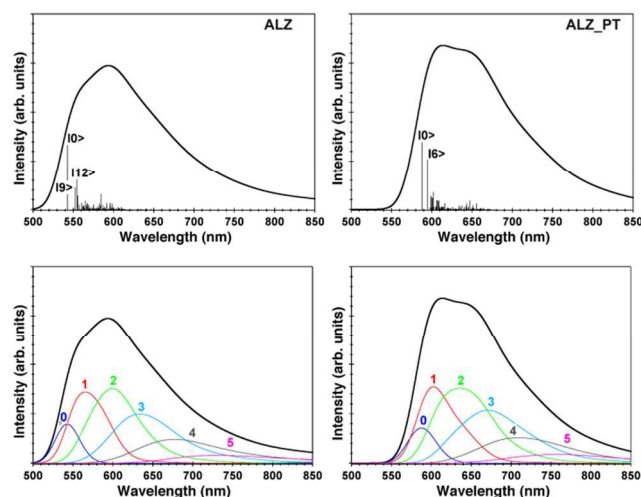

Figure 4 . Emission spectra computed in benzene of ALZ (left) and ALZ_PT (right) with the main vibronic transitions involved (top) and decomposition of the spectra in contributions from the 0-0 transition (0) and the n (n=1,5) simultaneously excited oscillators (bottom).

The isodensity plots of the HOMO/LUMO involved in the lowest transition of ALZ and ALZ_PT are reported in the right side of Figure 3. The HOMO of ALZ is mainly localized on the A ring, that one of ALZ_PT is similar with the addition of charge delocalization between C_2-C_1 in C-ring and the C_{10} in B-ring, reflecting the major conjugation of the proton transfer tautomer. The LUMO of both tautomers are completely delocalized over the molecules. The HOMO→LUMO transition, which gives rise to the absorption spectra, has therefore a mixed π-π^* and charge transfer (CT) character, the electron density moving from the A-Ring to the B and C-rings. The HOMO/LUMO orbitals for ALZ_PT species are destabilized/stabilized with respect to ALZ thus lowering the HOMO-LUMO gap that is reflected in a red-shift of the main absorption band. The absorption maxima of ALZ_PT spectra are computed red-shifted by ca. 0.4 eV compared to ALZ.

Vibrationally resolved emission spectra

To fully characterize the emission process of alizarin and the involvement of both the tautomers, we computed the vibrationally resolved emission spectra of ALZ and ALZ_PT in benzene and in ethanol. We consider the emission coming from the minima molecular structures obtained from the S_1 SS curves (Figure 2). Vertical emissions computed for the optimized LR-PCM geometries (Figure 1) have also been computed and are reported in ESI.

The ALZ emission spectrum computed in benzene, see Figure 4 (left, top), shows a maximum at 595 nm, a shoulder blue-shifted with respect to the emission maximum at ca. 560 nm and a long tail at low energies. The emission peak is mainly due to transitions of double simultaneously excited oscillators with minor contributions of single and triple excited oscillators, see Figure 4 (left, bottom). The shoulder at 560 nm is due to the 0-0 transition and to transitions of single excited oscillators, being the most intense the <0|9> and <0|12> transitions. The tail at low energies is instead due to the triple transitions with a minor contribution from 2 and 4 simultaneously excited oscillators
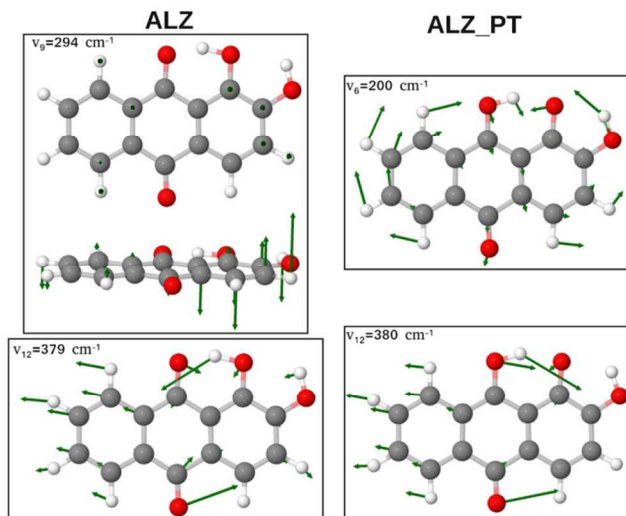
Figure 5 Vibrational modes ν_9 (top) and ν_{12} (bottom) for ALZ (left) and vibrational modes ν_6 (top) and ν_{12} (bottom) for ALZ_PT computed in benzene**.**

Figure 6 . Computed emission spectra in benzene (top) and ethanol (bottom) of ALZ (red;1) and ALZ_PT (black;2). Top panel inset: experimental emission spectra in benzene at different excitation wavelengths from ref. [44]. Bottom panel inset experimental spectra in acetonitrile (1), ethanol (2) and benzene (3) from ref. [44].

transitions. Mode ν_9 at 294 cm^{-1} corresponds to an out-of-plane boat-like vibration of the external rings, manly C-ring, see Figure 5, while mode ν_{12} at 379 cm^{-1} corresponds to the two carbonyl bending and to C_1OH bending in phase with the C=O bending plus a breathing of the A-Ring. This latest vibrational mode drives the alizarin tautomerization by assisting the inter-molecular proton transfer decreasing the $O_{10}H$ distance.

The shape of the emission spectrum computed for ALZ_PT in benzene is quite similar to that of ALZ though red-shifted and slightly more intense. We computed two bands at 610 and 645 nm and a long tail at low energies, see Figure 4 (right, top). The band at higher energies is slightly more intense than the band at 645 nm, contrarily to what computed for ALZ. The band at 610 nm is formed by the 0-0 transition and single quanta transitions, in particular <0|6> and <0|12>. On the other hand, the band at 645 is mainly due to double and triple excited oscillator transitions and the low energy tail is essentially due to triple and quadruple excited oscillator transitions, see Figure 4 (right, bottom). Vibrational normal mode ν_6 is computed at 200 cm^{-1} and manly accounts for the rigid bending of A and C-rings towards the axis formed by the two carbonyls of ring B, the ν_{12} computed at 380 cm^{-1} is equivalent to the ν_{12} mode computed for ALZ and assists the back-proton transfer, see Figure 5.

Experimentally in benzene a double emission has been measured for alizarin and has been ascribed to the deactivation of both tautomers. As already discussed in previous sections, the computed similar stability for ALZ and ALZ_PT along with the small barrier associated to the proton transfer would suggest that both the lowest excited states of ALZ and ALZ_PT should be populated. Therefore, it is reasonable to hypothesize that the emission spectrum might be the result of the fluorescence spectra of both tautomers whose contribution depends on their relative distribution given by their relative stabilities that determine the number of molecules that have been allowed to overcome the barrier at a given excitation wavelength. Figure 6 (top) reports the vibrationally resolved emission spectra in benzene of ALZ and ALZ_PT with the corresponding transitions compared to the available experimental data.
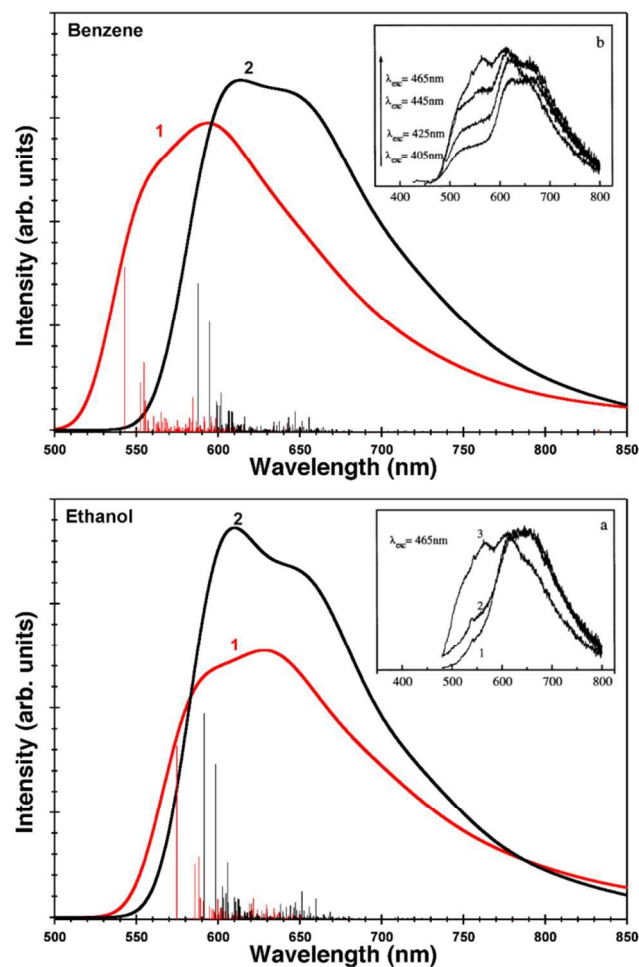
The results computed in benzene are compatible with the experimental picture from ref. [44] and the simulated spectrum that would come from a combination of the ALZ and the ALZ_PT is in good agreement in terms of energy with the experimental data. When exciting at high energy, 405 nm (3.06 eV), a larger ratio of the molecules overcomes the barrier and emit from the ALZ_PT tautomer increasing the relative intensity of the emission band between 620-690 nm (2.03-1.80 eV). This band is in excellent agreement, within 0.05 eV, with the theoretical emission of ALZ_PT that is computed between 600-660 nm (2.00-1.85 eV). On the other hand, exciting at lower energy 465 nm (2.66 eV) the emission from the ALZ tautomer increases and two distinguishable bands are measured; the band at high energy is reproduced by the signal computed for ALZ (0-0 and singles) while the experimental emission maximum at 610 nm is described by contributions from both the low energy band of ALZ (doubles) and the high energy band of ALZ_PT (0-0 and singles).

For alizarin, in polar solvents as ethanol and acetonitrile, a single broad emission band at ca. 640 nm was measured in contrast with the double band retrieved in benzene, thus hypothesising a higher barrier height and an emission coming only from the proton

transfer tautomer for polar solvents.[41] Our computed relative stabilities estimated from the SS approach suggest that the ALZ is more stable than the ALZ_PT species in polar solvents, and that a quite high energy barrier is associated to the proton transfer process (3.19 kcal/mol). However, results in ethanol might be affected by an incomplete treatment of the solvent effects with the continuum polarizable model used in this investigation. Bearing this in mind, we can not exclude from our calculations the presence of none of the tautomers; Figure 6 (bottom) reports the computed emission in ethanol for both tautomers. The composition of the computed emission spectra in ethanol in terms of classes and transitions contributions is essentially the same as in benzene and is therefore reported only in ESI.

Comparing the emission spectra of Figure 6 it can be observed that while that of ALZ_PT is essentially unchanged with the increase of the solvent polarity, the ALZ spectrum is red-shifted with respect to its benzene counterpart. The emission spectrum of ALZ_PT is more intense than that of ALZ, as already observed in benzene, even though the ratio between the intensity is higher in ethanol. The emission energies computed using PBE0 and M06 functionals (see ESI for further details), show only a rigid shift of ca. 0.10 eV with respect to the B3LYP ones, and confirm the different behaviour retrieved for the tautomers emissions in polar/non ploar solvents.

We notice from the bottom panel of Figure 6 that the computed emission spectra of ALZ and ALZ_PT tautomers lay in the same spectral region and are both compatible with the experimental emission, both in terms of energy and spectral shape, presenting a plateau-like maximum between 590 and 670 nm. Therefore, no definitive conclusions regarding the species present in polar solvents can be inferred from calculations. Experimental spectra would be compatible with an emission coming from ALZ only, ALZ_PT only or from a combination of both species though according to the relative stabilities computed and the estimated barrier associated to the proton transfer only ALZ should be in principle responsible for the emission spectrum. From our calculations we can exclude the double emission in polar solvents, independently by the relative tautomer stabilities.

Solvatochromism: the electronic factors

To explain the solvatochromism shown in emission by alizarin with respect to solvents of different polarity, we analyzed the electronic charge distribution of ALZ and ALZ_PT at the S_0 and S_1 geometries as a function of the media. Solvatochromism is a very complex phenomenon which gives a measure of a different response to the solvation effects of the dye charge distribution at the ground and first excited state.[64,65] These effects can be specific or not-specific depending on the nature of the solvent (protic/non protic solvents) and on its dielectric constant (polar/non polar solvents). The change of charge distribution between ground and excited states can be roughly monitored by analyzing the dipole moment of the ground and lowest excited states, $\mu(S_0)$ and $\mu(S_1)$, even though dynamical effects should be properly taken into account.[65] For alizarin the presence of the proton transfer tautomer (ALZ_PT) at the lowest excited state makes the interpretation picture even more complex.

To find a rationale for the alizarin solvatochromism, we therefore computed the $\mu(S_0)$ and $\mu(S_1)$ of both ALZ and ALZ_PT

Table 2 Dipole moments (Debye) for the ground and first excited states.

	ALZ		ALZ_PT	
	μ S_0 (S_1)	Δμ $_{S1-S0}$	μ S_0 (S_1)	Δμ $_{S1-S0}$
Vacuo[a]	2.03 (2.77)	0.74	2.85 (0.66)	-2.19
Benzene[b]	2.31 (3.94)	1.63	3.29 (0.76)	-2.53
Ethanol[b]	2.64 (5.06)	2.42	3.82 (0.98)	-2.84

[a] S_0 and S_1 computed on the optimized structures. [b] S_0 computed on the optimized structures, S_1 computed using SS-PCM procedure on the minima structures from the S1 SS curve (Figure 2).

species; for the ground state we refer to the optimized structure, while for the excited state structure we refer to the minima of the SS-PCM curve reported in Figure 3. The computed dipole moments in the different considered media along with the differences between the lowest excited state dipole moment and the ground state dipole moment (Δμ S_1-S_0) are reported in Table 2. For ALZ, $\mu(S_0)$ in vacuo is ca. 2.0 D while in the excited state increases up to ca. 2.8 D. While the $\mu(S_0)$ weakly changes with respect to the different media (0.61 D from vacuo to ethanol), a more polar S_1 structure is stabilized in ethanol, the $\mu(S_1)$ passing from 2.77 D (vacuo) to 5.06 D (ethanol).

The ALZ_PT $\mu(S_0)$ varies similarly to that of ALZ increasing by 0.97 D passing from vacuo to ethanol, while $\mu(S_1)$ has a different behaviour markedly decreasing with respect to that of the ground state by a factor 3, and being slightly affected by the medium, passing from 0.66 D (vacuo) to 0.98 D (ethanol). From the analysis of the Δμ(S_1 -S_0), which can be roughly related to the sovatochromism, we found that ALZ shows a marked increase of the difference between the dipole moment of S_0 and S_1 by increasing the solvent polarity. On the other hand, for the ALZ_PT species we computed a similar Δμ(S_1-S_0) independently on the solvent polarity, and with an opposite sign with respect to ALZ. On overall, our results highlight the two tautomers intrinsically respond to solvents of different polarity in a completely different way: (i) in ALZ the more polar excited state is more stabilized by polar solvent than the ground state showing a positive solvachromism; (ii) in ALZ_PT the ground state is more polar than S_1 state and is stabilized in polar solvent thus showing a weak negative solvatochromism.

The different charge distribution of ground and excited states of ALZ and ALZ_PT implies different stabilization of the two S_0 and S_1 states in different solvents further explaining the computed emission behaviour. In fact the two tautomers oppositely behave in different solvents showing for ALZ a red shift in ethanol with respect to vacuo and benzene, while ALZ_PT does not change the emission wavelength from vacuo to ethanol.

Summary and Conclusions.

DFT and TDDFT have been employed to study the photophysical and photochemical properties of alizarin, a widely investigated fluorescent organic dye, focusing our attention on its optical properties in relation to an excited state internal proton transfer. We have focused our attention on the photophysics of the excited state of interest (S_1) to rationalize the emission process in solvents of different polarity. Geometry optimizations and frequency calculations using LR-PCM have confirmed that both ALZ and ALZ_PT are stable in S_1. ALZ_PT tautomer is more stable by 1.40 kcal/mol than ALZ in benzene while in ethanol ALZ is more stable by only 0.20 kcal/mol. The potential energy

curves of the ESIPT obtained equilibrating the solvent on the LR-optimized geometries substantially differ from their LR counterparts. LR potential energy curves show no clear barrier height and a flat zone around 1.3 Å $O_{10}H$ distance and they are
5 very similar in both solvents. Interestingly, equilibration of the solvent leads in benzene to a real minimum for each tautomer and a barrier height of ca. 2 kcal/mol while in ethanol, ALZ is computed ca. 1.9 kcal/mol more stable than ALZ_PT.

The small computed energy differences suggest an equilibria of
10 both forms in the two different solvents. The vertical emission excitations computed show that ALZ_PT emission is red-shifted between 0.27 and 0.13 eV with respect to that of ALZ. The ALZ_PT emission energies are almost insensitive to the solventt polarity, while the ALZ ones are red-shifted when passing from
15 benzene to ethanol.

The vibrationally-resolved emission spectra computed for ALZ and ALZ_PT have similar shapes with two distinguishable. On overall, the ALZ_PT spectrum is more intense and red-shifted with respect to that of ALZ but in benzene the red shift is large
20 and the two spectra are clearly distinguishable. In benzene both ALZ and ALZ_PT species contribute to the emission, the result is an emission spectrum which accounts for the spectral features of both tautomers emission spectra. The wavelength dependent double emission measured[44] is compatible with the presence of
25 two stable tautomers in the excited state and the computed spectra of both tautomers are in good agreement with the retrieved experimental bands. When exciting at high energy a larger ratio of the molecules overcomes the barrier and emit from the ALZ_PT tautomer, increasing the relative intensity of the
30 experimental emission band retrieved between 610 and 690 nm. On the other hand, the experimental band between 525 and 575 nm is compatible with the computed spectra of the ALZ tautomer. This signal would increase when exciting at lower energies resulting in a double band emission spectra with peaks
35 centered at 610 and 540 nm corresponding to emissions coming from both ALZ_PT and ALZ and from only ALZ, respectively.

A more complex picture is found for ethanol, where the emission of ALZ is computed red-shifted with respect to that in bezene, resulting in emission spectra that lay in the same region.for both
40 tautomers. Therefore, from the comparison between the computed and experimental spectra is not possible to rule out the presence of one or the other tautomer.

The ground state and excited state dipole moments strongly vary for ALZ going from benzene to ethanol, showing a marked
45 sovatochromism of the emission, while the two dipole moments undergo more slight changes for ALZ_PT. Including energy considerations, from our calculations only the ALZ species is responsible of the emission spectrum and this species by its own is able to explain the measured emission spectrum. The analysis
50 of the variation of the dipole moment of S_0 and S_1 in solvents of different polarity allows us to relate the different solvatochromic behaviour of the two tautomers to a larger increase of charge polarization in the ALZ S_1, which therefore results more stabilized in polar solvents than ground state.

55 Results obtained for alizarin show that the recent advances in computational chemistry have allowed to achieve a such accuracy in the excited state computed properties almost comparable to that obtained for the ground state. Our calculations on the

emission spectra of alizarin are in good agreement with the
60 experimental data reproducing the trend of the experimental fluorescence with the increase of the excitation energy and with the changes on the solvent polarity.

Notes and references

[a]Computational Laboratory for Hybrid/Organic Photovoltaics (CLHYO), CNR-ISTM, Via Elce di Sotto 8, I-06123, Perugia, Italy, Fax: +39 075 585 5606; Tel: +39 075 585 5618/+39 075 585 5522; E-mail:
70 anna@thch.unipg.it, simona@thch.unipg.it
[b]CNR-ISTM, Via Elce di Sotto 8, I-06123, Perugia, Italy, Fax: +39 075 585 5606; Tel: +39 075 585 5639; E-mail: costanza.miliani@cnr.it
[c]Centro di Eccellenza SMAArt (Scientific Methodologies applied to Archaeology and Art), Dipartimento di Chimica, Biologia e
75 Biotecnologie, Università di Perugia, via Elce di Sotto 8, IT-06123, Italy, Tel: +39 075 585 5620; E-mail: romani@unipg.it

References

1 M. Hovaneissian, P. Archier, and C. Vieillescazes, *Dyes and Pigments*, 2007, **74**, 706.
85 2 D.S. Alves, L. Perez-Fons, A. Estepa, and V. Micol, *Biochemical Pharmacology*, 2004, **68**, 549.
3 S.A. Norton, *J. of the Am. Academy of Dermatology*, 1998, **39**, 484.
4 A.D. Dixon, and D.A.N. Hoyte, *The Anatomical Rec.*, 1963, **145**, 101.
90 5 R. de la Rie, *Stud. Conserv.* 1982, **27**, 1; R. de la Rie, *Stud. Conserv.* 1982, **27**, 65, R. de la Rie, *Stud. Conserv.* 1982, **27**, 102.
6 M. Matteini and A. Moles, La Chimica nel Restauro. Nardini: Florence, 1986.
7 P. Novotna, V. Pacakova, Z. Bosakova, and K. Stulik, *J. of Chromat. A*, 1999, **863**, 235.
95
8 J. Orska-Gawrys, I. Surowiec, J. Kehl, H. Rejniak, K. Urbaniak-Walczak, and M. Trojanowicz, *J. of Chromat. A*, 2003, **989**, 239.
9 B. Szostek, J. Orska-Gawrys, I. Surowiec, and M. Trojanowicz, *J. of Chromat. A*, 2003, **1012**, 179.
100 10 J. Wouters and N. Rosario-Chirinos, *J. of the Am. Inst. for Cons.*, 1992, **31**, 237.
11 W. R Duncan, O. V. Prezhdo, *Annu. Rev. Phys. Chem.*, 2007, **58**, 143
12 W. R Duncan, W. M.; Stier, and O. V. Prezhdo, *J. Am. Chem. Soc.*, 2005, **127**, 7941
105 13 A. Nawrocka and S. Krawczyk, *J. Phys. Chem. C*, 2008, **112**, 10233.
14 W. R Duncan and O. V. Prezhdo, *J. Phys. Chem. B*, 2005, **109**, 365.
15 W. R Duncan, C. F. Craig and O. V. Prezhdo, *J. Am. Chem. Soc.,* 2007, **12**, 8528
16 W. R Duncan and O. V. Prezhdo, *J. Am. Chem. Soc.,* 2008, **130**,
110 9756
17 S. Kaniyankandy, S. Verma, J. A. Mondal, D. K. Palit and H. N. Ghosh, *J. Phys. Chem. C*, 2009, **113**, 3593.
18 R. Sánchez-de-Armas, M. A. San-Miguel, J. Oviedo and J. Fdez. Sanz, *J. Chem. Theory, Comput.*, 2010, **6**, 2856.
115 19 J. Li, I. Kondov, H. Wang and M. Thoss, *J. Phys. Chem C*, 2010, **114**, 18481.
20 Y Di Iorio, M. A. Brusa, A. Feldhoff, and M. A. Grela, *ChemPhysChem*, 2009, **10**, 1077.
21 C. Bernini, L. Zani, M. Calamante, G. Reginato, A.Mordini, M.
120 Taddei, R. Basosi and A. Sinicropi, *J. of Chem. Theory and Comp* **2014**, 10, 3925.
22 A. Amat, C. Clementi, C. Miliani, A. Romani, A. Sgamellotti and S. Fantacci, *Phys. Chem. Chem. Phys.* **2010**, 12, 6672.

23 A. Amat, C. Clementi, F. De Angelis, A. Sgamellotti, S. Fantacci, *J. Phys. Chem. A* **2009**, 113, 15118.

24 F. De Angelis, S. Fantacci, E. Mosconi, M. K. Nazeeruddin and M. Grätzel, *J. Phys. Chem. C* **2011**, 115, 8825.

25 F. De Angelis, S. Fantacci, R. Gebauer, R., *J. Phys. Chem. Lett.* **2011**, 2, 813.

26 G. Scalmani, M. J. Frisch, B. Mennucci, J. Tomasi, R. Cammi and V. Barone, *J. Chem. Phys.*, 2006, **124**, 094107.

27 R. Improta, V. Barone, and F. Santoro, *J. Phys. Chem. B*, 2007, **111**, 14080.

28 R. Improta, F. Santoro, and V. Barone, *Angew. Chem. Int. Ed.* 2007, **46**, 405.

29 F. Santoro, R. Improta, A. Lami, J. Bloino, and V. Barone, *J. Chem. Phys.*, 2007, **126**, 084509.

30 F. Santoro, A. Lami, R. Improta, and V. Barone, *J. Chem. Phys.*, 2007, **126**, 184102.

31 F. Santoro, A. Lami, R. Improta, J. Bloino, and V. Barone, *J. Chem. Phys.*, 2008, **128**, 224311.

32 V. Barone, J. Bloino, M. Biczysko, and F. Santoro, J. *Chem. Theory and Comput.*, 2009, **5**, 540.

33 J. Preat, A. D. Laurent, C. Michaux, E. A. Perpète and D. Jacquemin, *J. Mol. Struc. (THEOCHEM)*, 2009, **901**, 24.

34 M. Savko, S. Kascakova, Peter Gbur, P. Miskovsky and J. Ulicny, *THEOCHEM*, 2007, **823** 78-86 .

35 P. Cysewski, T. Jelinski, M. Przybyeka and A. Shyichukb , *New J. Chem.*, 2012, **36**, 1836-1843.

36 L. Carta, M. Biczysko, J. Bloino, D. Licari and V. Barone Phys. Chem. Chem. Phys., 2014, **16**, 2897.

37 I. Kondov, H. Wang and M. Thoss, *Int. J. of Quant. Chem.*, 2006, **106**, 1291.

38 N. Komiha, O. K. Kabbaj and M. Chraibi, *J. Mol. Struc. (THEOCHEM)*, 2002, **594**, 135.

39 S. Say-Liang-Fat and J. P. Cornard, *Polyhedron*, 2011, **30**, 2326.

40 A. Lapini, P. Fabbrizzi, M. Piccardo, M. di Donato, L. Lascialfari, P. Foggi, S. Cicchi, M. Biczysko, I. Carnimeo, F. Santoro, C. Cappelli and R. Righini, *PCCP*, 2014, **16**, 10059.

41 C. Miliani, A. Romani and G. Favaro, *J. Phys. Org. Chem*, 2000, **13**, 141.

42 R.C. Weast, Handbook if Chemistry and Physics, 51ˢᵗ Ed, The Chemical Rubber Company, Ohio, 1970.

43 R.H. Thomson, Naturally occurring Quinones, 2ⁿᵈ Ed., Academic Press, London, 1971.

44 C. Miliani, A. Romani and G. Favaro, *Spectrochimica Acta Part A*, 1998, **54**, 581.

45 C. Grazia, C. Clementi, C. Miliani and A. Romani, ***Photochem. & Photobiol. Sci.,*** 2011, **10**, 1249-1254**.**

46 J. Tomasi, B. Mennucci and R. Cammi, *Chem. Rev.*, 2005, **105**, 2999.

47 R. Improta, G. Scalmani, M. J. Frisch and V. Barone, *J. Chem. Phys.*, 2007, **127**, 074504.

48 R. Improta, V. Barone, G. Scalamani and M. J. Frisch, *J. Chem Phys*, 2006, **125**, 054103.

49 P. Hohenberg and W. Kohn, *Phys. Rev.*, 1964, **136**, B864.

50 R. E. Stratmann, G. E. Scuseria and M. J. Frisch, *J. Chem. Phys.*, 1998, **109**, 8218.

51 R. Bauernschmitt and R. Ahlrichs, *Chem. Phys. Lett.*, 1996, **256**, 454.

52 M. E. Casida, C. Jamorski, K. C. Casida and D. R. Salahub, *J. Chem. Phys.*, 1998, **108**, 4439.

53 Gaussian 09, Revision A.2, M. J. Frisch, G. W. Trucks, H. B. Schlegel, G. E. Scuseria, M. A. Robb, J. R. Cheeseman, G. Scalmani, V. Barone, B. Mennucci, G. A. Petersson, H. Nakatsuji, M. Caricato, X. Li, H. P. Hratchian, A. F. Izmaylov, J. Bloino, G. Zheng, J. L. Sonnenberg, M. Hada, M. Ehara, K. Toyota, R. Fukuda, J. Hasegawa, M. Ishida, T. Nakajima, Y. Honda, O. Kitao, H. Nakai, T. Vreven, J. A. Montgomery, Jr., J. E. Peralta, F. Ogliaro, M. Bearpark, J. J. Heyd, E. Brothers, K. N. Kudin, V. N. Staroverov, R. Kobayashi, J. Normand, K. Raghavachari, A. Rendell, J. C. Burant, S. S. Iyengar, J. Tomasi, M. Cossi, N. Rega, J. M. Millam, M. Klene, J. E. Knox, J. B. Cross, V. Bakken, C. Adamo, J. Jaramillo, R. Gomperts, R. E. Stratmann, O. Yazyev, A. J. Austin, R. Cammi, C. Pomelli, J. W. Ochterski, R. L. Martin, K. Morokuma, V. G. Zakrzewski, G. A. Voth, P. Salvador, J. J. Dannenberg, S. Dapprich, A. D. Daniels, Ö. Farkas, J. B. Foresman, J. V. Ortiz, J. Cioslowski, and D. J. Fox, Gaussian, Inc., Wallingford CT, 2009.

54 A. D. Becke, J. Chem. Phys., 1993, **98**, 5648.

55 C. Lee, W. Yang and R. G. Parr, *Phys. Rev. B: Condens. Matter*, 1988, **37**, 785.

56 B. Miehlich, A. Savin, H. Stoll and H. Preuss, *Chem. Phys. Lett.*, 1989, **157**, 200.

57 V. A. Rassolov, M. A. Ratner, J. A. Pople, P. C. Redfern and L. A. Curtiss, *J. Comput. Chem.*, 2001, **22**, 976.

58 V. A. Rassolov, J. A. Pople, M. A. Ratner and T. L. Windus, *J. Chem. Phys.*, 1998, **109**, 1223.

59 A. Le Person, J. P. Cornard, S. Say-Liang-Fat, Chem. Phys. Lett. 2011, **517**, 41-45.

60 M. Shamsipur, T. Poursaberi, A. Avanes, abd H. Sharghi, *Spectrochim. Acta A*, 2006, **63,** 9.

61 C. Adamo, V. Barone, *J. Chem. Phys.*, 1999, **110**, 6158-6169.

62 Y. Zhao, D. G. Truhlar, *Theor. Chem. Acc.*, 2008, **120**, 215-241.

63 Y. Zhao, D. G. Truhlar, *Chem. Phys. Lett*., 2011, **502**, 1-13.

64 M. Homocianu, Anton Airinei, D. Ortansa Dorohoi, *J. of Adv. Res. in Phys.*, 2011, **2**, 011105.

65 A. Marini, A. Munoz-Losa, A. Biancardi, B. Mennucci, *J. Phys. Chem. B*, 2010, **114**, 17128–17135
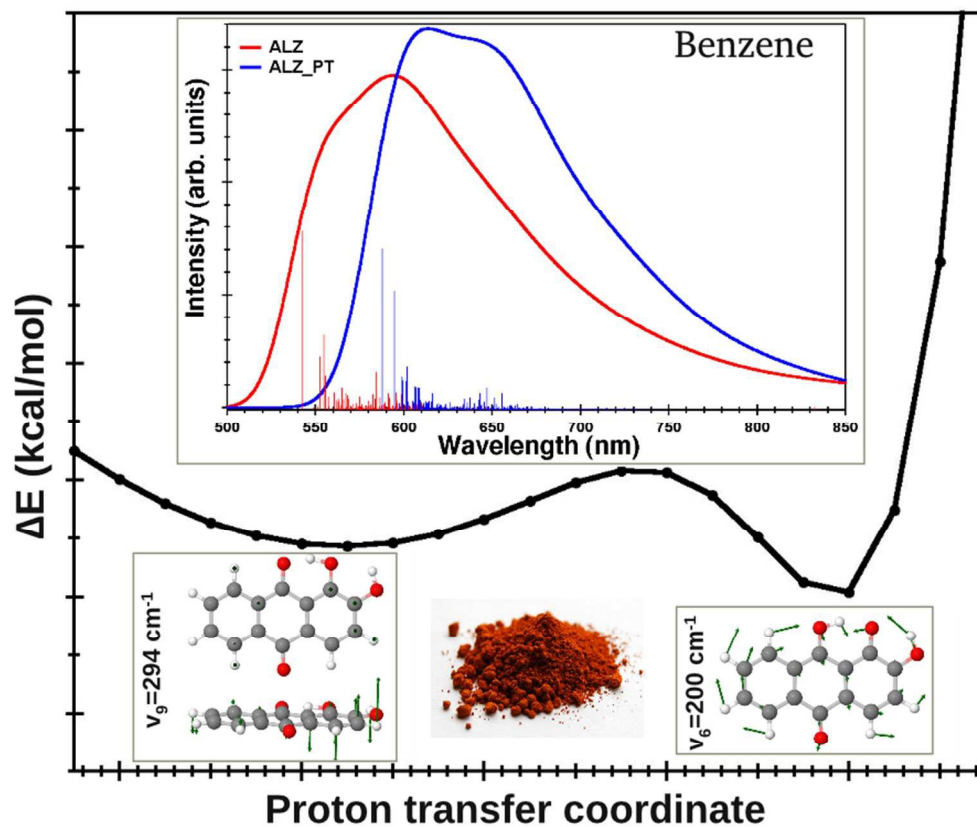
Potential energy curve for the ESIPT. Top Inset: Vibrationally resolved emission computed for both tautomers. Bottom inset: main vibrational modes.